

# Carrier Recovery Techniques on Satellite Mobile Channels

B. Vucetic

and

J. Du

Department of Electrical Engineering, Sydney University

Sydney 2006, Australia

Phone: 61-2-6923514

Fax: 61-2-6923847

## Abstract

An analytical method and a stored channel model were used to evaluate error performance of uncoded QPSK and MPSK trellis coded modulation (TCM) over shadowed satellite mobile channels in the presence of phase jitter for various carrier recovery techniques.

## 1 Introduction

In coherent digital transmission systems accurate carrier phase and symbol timing information are essential for successful demodulation. The reconstruction of coherent reference can be accomplished in many ways. In general, carrier and clock are restored by pilot tone and self-synchronizing techniques. Self-synchronizing methods could be quite roughly divided into decision-directed algorithms and feedforward nonlinear phase estimators. This paper compares three representatives of the above classes and analyzes their relative merits on satellite mobile channels with shadowing. The impact of phase jitter on coherently demodulated QPSK and M-PSK trellis coded modulation (TCM) with feedforward (FF), decision directed (DD) and TTIB techniques for carrier phase recovery on a is considered.

A stored experimental channel [2] was used to simulate the performance of a satellite mobile communication system. The experimental data for the stored channel were obtained in land mobile satellite propagation measurements at L band in Syd-

ney suburban areas via the Japanese ETS-V and INMARSAT-POR geostationary satellites.

## 2 System Model

### 2.1 System Description

In the systems under consideration a voice codec generates data digits at a rate of  $1/T_b$ . If the QPSK modulation is used the 2-bit input sequences modulate a QPSK waveform at a rate  $1/2T_b$  symbols/s. In the 8-PSK TCM system the binary sequence is encoded in a rate  $2/3$  convolutional encoder. The 3-bit symbols at the output of the encoder are then block interleaved and used to modulate an 8-PSK waveform at a rate  $1/2T_b$  symbols/s according to the set partitioning rules [6]. The interleaver size is chosen on the order of the worst case fade depth in the simulations and assumed infinite in the analysis. We consider three different methods for carrier phase recovery, FF, DD and TTIB techniques.

### 2.2 Model of Shadowed Channel

The signal in a shadowed channel is obtained as the sum of a lognormally distributed random phasor  $ye^{j\phi_0}$  and a Rayleigh phasor  $we^{j\phi}$  :

$$ae^{j\theta} = ye^{j\phi_0} + we^{j\phi} \quad y, w > 0$$

where the phases  $\phi_0$  and  $\phi$  are uniformly distributed between 0 and  $2\pi$ .

The conditional probability of a given  $y$  is Rician:

$$p(a | y) = \frac{a}{\sigma_r^2} \exp\left(-\frac{r^2 + y^2}{2\sigma_r^2}\right) I_0\left(\frac{ay}{\sigma_r^2}\right)$$

where  $2\sigma_r^2$  represents the average scattered power due to multipath propagation.

The total probability is given by

$$p(a) = \int_0^\infty p(a | y)p(y)dy$$

It is assumed that  $p(y)$  is lognormally distributed:

$$p(y) = \begin{cases} \frac{1}{\sqrt{2\pi\sigma_1 y}} \exp\left(-\frac{(\ln y - \mu)^2}{2\sigma_1^2}\right) & 0 \leq y < \infty \\ 0 & \text{otherwise} \end{cases}$$

with the mean

$$\mu_y = E\{y\} = \exp(\mu + \sigma_1^2/2)$$

and the variance

$$\sigma_y^2 = E\{(y - \mu_y)^2\} = \exp(2\mu + \sigma_1^2) (\exp(\sigma_1^2) - 1)$$

### 3 Phase Estimation in FF Technique

Let us assume that  $v_i$  represents an MPSK symbol sample transmitted at time  $i$ . The phase of the  $i$ th transmitted sample can be written as

$$\alpha_i = k_i \frac{2\pi}{M}$$

where  $k_i$  is an integer ( $k_i \in \{0, 1, \dots, M-1\}$ ).

The corresponding received sample at the input of the coherent demodulator is:

$$r_i = a_i v_i + n_i$$

where  $a_i$  is a real random variable equal to the envelope of the channel attenuation normalized to the transmitted signal,  $n_i$  is a sample of a zero mean complex additive white Gaussian noise (AWGN). The received sample can be expressed as

$$r_i = r_{Ii} + jr_{Qi} = \rho_i \exp(j\phi_i)$$

$$\rho_i = \sqrt{r_{Ii}^2 + r_{Qi}^2}$$

and

$$\phi_i = \tan^{-1} \frac{r_{Qi}}{r_{Ii}}$$

On the other hand the received sample phase can be expressed as

$$\phi_i = \alpha_i + \varphi_i + \epsilon_i$$

where  $\varphi_i$  is the phase jitter and  $\epsilon_i$  is the phase error caused by Gaussian noise.

In the FF algorithm for each sample we multiply the phase  $\phi_i$  by  $M$  and perform a nonlinear transformation  $F$  on the amplitude  $\rho_i$  [8]. As the result we obtain the signal

$$r'_{Ii} + jr'_{Qi} = F(\rho_i) \exp(jM\phi_i)$$

The phase of the resulting signal is

$$M\phi_i = M\alpha_i + M\theta_i = 2k_i\pi + M\theta_i$$

The phase error  $\theta$  is then estimated over  $2N + 1$  symbols as

$$\theta = \frac{1}{M} \tan^{-1} \frac{\sum_{i=-N}^N \rho_i \sin M(\epsilon_i + \varphi_i)}{\sum_{i=-N}^N \rho_i \cos M(\epsilon_i + \varphi_i)} \quad (1)$$

$\theta$  represents the phase by which the corresponding symbol is rotated.

The above operations cause an  $M$ -fold ambiguity in the phase estimate. It can be resolved by differential decoding for  $M$ -PSK modulation and  $2\pi/M$  phase rotationally invariant  $M$ -PSK modulation. If non-rotationally invariant codes are used the phase ambiguity can be removed by monitoring Viterbi decoder metrics.

### 4 Phase Estimation in DD Technique

The DD is a recursive algorithm which is used for both phase and symbol timing estimation [4]. The algorithm operates under the assumption that the incoming symbols are known to the receiver. This condition is met for small error probabilities or alternately if some known pattern sequence is transmitted in a training period.

If the current phase estimate is  $\theta_i$  the next symbol phase rotation is determined as

$$\theta_{i+1} = \theta_i + \Gamma \text{Im}\{r_i \hat{r}_i^*\} \quad (2)$$

where  $\Gamma$  is a small number determined to achieve a trade-off between the phase error and the convergence rate and  $\hat{r}_i$  is the  $i$ th sample estimate.

The symbol sampling time is determined by using a second order digital filter. The sampling time sequence  $\{\tau_i\}$  is determined as

$$\tau_{i+1} = \tau_i + \lambda \text{Re}\{r_i r_{i-1}^* - r_{i-1} r_i^*\} \quad (3)$$

where  $\lambda$  is a small number.

The phase error can be approximated as

$$\theta_{i+1} \simeq \Gamma(\epsilon_i + \varphi_i) \quad (4)$$

where  $\epsilon_i$  is the phase noise induced by Gaussian noise and  $\varphi_i$  is the phase jitter.

In block structured data transmission the performance of the algorithm can be improved by sending a preamble at the beginning of each block [5].

## 5 Phase Estimation in TTIB Technique

The filtering in the TTIB algorithm is achieved by using two bandpass filters with a combined frequency response equivalent to a square root raised cosine transfer function [7]. Each bandpass filter is used to isolate one of two subbands with bandwidths equal to one half of the symbol transmission rate. The subband signals are further frequency translated to enable the insertion of the pilot tone. The bandstop margin is chosen large enough to accommodate the worst case Doppler shift and meet the acquisition time requirements of the receiver. The reference tone is positioned centrally within the signal bandwidth to assure an accurate estimation of the signal degradation.

In the TTIB demodulator the received pilot tone is used to remove phase error. This process is accomplished by computing the pilot tone phase and multiplying each symbol by the negative pilot tone phase. It is essential to choose an appropriate pilot tone level and filter bandwidths. As the pilot tone level increases more power is wasted on the tone transmission. On the other hand if the pilot tone power is reduced, it will degrade its signal-to-noise ratio and phase estimate. Similarly, the pilot tone bandwidth has an optimum. In order to reduce the impact of Gaussian noise it is desirable to have a small pilot tone bandwidth. However, the bandwidth is determined by maximum Doppler shifts in the channel to enable pilot tone extraction.

The insertion of pilot tone, however, will result in a non-constant envelope signal and degrade the performance of this algorithm on a nonlinear channel.

The BER degradation on a satellite channel with a TWT nonlinear amplifier is of the order of 0.5 dB [1].

## 6 Probability of Error for QPSK

The conditional bit error probability for QPSK modulation given the fading attenuation due to shadowing  $a$  and the phase jitter  $\theta$  is given by

$$P_{bc} = Q\left(\frac{a \cos \theta}{\sigma}\right)$$

where  $\sigma$  is the variance of the Gaussian noise in each signal space coordinate.

The total bit error probability is given by

$$P_b = \int_0^\infty \int_{-\pi}^\pi Q\left(\frac{a \cos \theta}{\sigma}\right) p(a) P(\theta) da d\theta$$

where  $p(a)$  and  $p(\theta)$  are the probability distributions of fading attenuation and phase jitter, respectively.

## 7 Error probability for TCM Schemes

Let  $C$  denote the set of all possible coded signal sequences  $\{z_N\}$ , where  $z_N$  is a coded symbol sequence of length  $N$ :

$$z_N = (z_1, z_2, \dots, z_i, \dots, z_N)$$

Let us assume that  $v_N$ :

$$v_N = (v_1, v_2, \dots, v_i, \dots, v_N)$$

an element of  $C$ , is the transmitted sequence. Then  $v_i$  represents the MPSK symbol transmitted at time  $i$ .

$$v_i = v_{Ii} + jv_{Qi}$$

where  $v_{Ii}$  and  $v_{Qi}$  are I and Q channel components, respectively.

For codes with large minimum number of symbols on error paths or for any code at small  $E_b/N_0$  the pairwise error probability can be upperbounded by [9]

$$P(v_N \rightarrow z_N) = P_{d,D,T} \leq \frac{1}{2} \frac{2\sigma d}{\sqrt{4\sigma^2 d^2 + \sigma_x^2}} \exp\left(-\frac{1}{2} \frac{m_x^2}{4\sigma^2 d^2 + \sigma_x^2}\right) \quad (5)$$

where

$$m_x = d^2 m_a m_{\theta 1} + T m_a m_{\theta 2}$$

$$T = \sum_{i=1}^N T_i \sum_{i=1}^N (z_{li} v_{Qi} - z_{Qi} v_{li})$$

and

$$\sigma_x^2 = D(m_{\theta 1^2} - m_a^2 m_{\theta 1}^2) + T_2(m_{\theta 2^2} - m_a^2 m_{\theta 2}^2)$$

$$D = \sum_{i=1}^N d_i^4$$

$$T_2 = \sum_{i=1}^N T_i^2$$

$$m_{\theta 1} = E[\cos\theta]$$

$$m_{\theta 1^2} = E[\cos^2\theta]$$

$$m_{\theta 2} = E[\sin\theta]$$

$$m_{\theta 2^2} = E[\sin^2\theta]$$

The bit error probability can be upperbounded by

$$P_b \leq \frac{1}{k} \sum_{d,D} b_{d,D,T} P_{d,D,T} \quad (6)$$

where  $b_{d,D,T}$  is the total number of erroneous information bits on all paths characterized by the Euclidean distance  $d$ , and the parameters  $D$  and  $T$ .

## 8 Results

The bit error rate performance with the QPSK modulation and FF algorithm relative to the demodulation without carrier recovery on a Gaussian channel with variable degrees of slowly varying phase jitter is given in Fig. 1. The algorithm removes almost completely the effect of phase jitter up to phase jitter values of  $30^\circ$ . The corresponding results for the 16-state Ungerboeck TCM code are illustrated in Fig. 2. The algorithm operates successfully up to phase jitter values of  $15^\circ$ . The impact of slowly varying phase jitter on the DD algorithm on a Gaussian channel is illustrated in Fig. 3. The algorithm is able to recover the signal phase up to  $40^\circ$  phase jitter. The BER for larger phase jitter exhibits high variations due to unreliable estimates of the signal phase. For a Gaussian channel with relatively low BER the algorithm works reliably and there is no need for transmission of preambles.

The performance of the TTIB technique depends on the pilot tone bandwidth. The pilot tone bandwidth should be chosen to match worst case Doppler shifts. For the ratio of the signal to the pilot tone

bandwidth  $\beta < 50$  the degradation is high. The sensitivity of the TTIB technique to phase jitter for QPSK and TCM is shown in Fig. 4. The TTIB algorithm can remove slowly varying phase errors, but cannot eliminate the effect of Gaussian noise due to finite pilot tone bandwidth. The loss for the QPSK is about 1dB for  $\beta = 50$ . For all TTIB tests the power of the pilot tone level was 10 dB below the total output power.

The comparative results of the three algorithms for the QPSK scheme on a satellite mobile shadowed channel are presented in Figure 5. The performance is evaluated by the average block error rate (BLER) which is a suitable parameter for digitized voice transmission, (the block length corresponds to 30ms frames). The DD algorithm requires accurate estimates of the received signal and the error performance is degraded by heavy shadowing. The additional information from a known received sequences can improve the reliability of signal estimation. Since the voice codec generally provides preambles at the beginning of each transmitted block of data it is possible to include this information in the DD algorithm. It should be noted that most degradation in the error rate comes from the amplitude variations rather than phase errors, since phase errors in the channel were generally less than  $10^\circ$ . Therefore, carrier recovery methods could not achieve significant performance improvement. Clearly, the TTIB technique shows the superior performance. However, an additional loss of about 2dB should be added due to the pilot tone transmission, nonlinearity and Doppler shift degradations.

The corresponding results for the 16-PSK TCM code is shown in Fig. 6.

## 9 Conclusions

An investigation of carrier recovery techniques on satellite mobile channels with shadowing has been performed.

The TTIB algorithm achieves the excellent phase estimates for low pilot tone filter bandwidth. accommodate the worst case Doppler shifts.

The DD algorithm with preamble transmission offers good performance, while the implementation is simple and the algorithm with the second order loop provides symbol timing and frequency tracking which is critical on mobile channels.

## 10 Acknowledgements

This work was carried with support from IR&D Board Grant No. 17001.

## References

- [1] Nicolas, J.J. and Vucetic B., Performance of MPSK Trellis Codes over Nonlinear Fading Mobile Satellite Channels, International Conference on Communication Systems, Conference Proceedings Singapore ICCS'88, pp.695-699, Singapore, November, 1988.
- [2] Data Files with I & Q data, AUSSAT
- [3] J.P. McGeehan and A.J. Bateman, Phase-Locked Transparent-Tone-in-Band (TTIB): A New Spectrum Configuration Particularly Suited to the Transmission of Data Over SSB Mobile Radio Networks, IEEE Trans. Comm. Techn., Vol. COM-32, Jan. 1984., pp. 81-87.
- [4] H. Kobayashi, Simultaneous Adaptive Estimation and Decision Algorithm for Carrier Modulated Data Transmission Systems, IEEE Trans. Commun. Tech., pp. 268-280, June 1971.
- [5] H.C. Guren, Burst Channel Receiver for Aeronautical Communications, ASSPA'89, Adelaide, Australia, 1989.
- [6] G. Ungerboeck, Channel Coding with Multi-level/Phase signals, IEEE Trans. Inform. Theory, vol. IT-28, Jan. 1982, pp. 55-67.
- [7] J.H. Lodge, M.L. Moher and S.N. Crozier, A Comparison of Data Modulation Techniques for Land Mobile Satellite Channels, IEEE Trans. on Vehicular Techn., vol. VT-36, No. 1., Feb. 1987, pp. 28-35.
- [8] A.J. Viterbi and A.M. Viterbi, Nonlinear Estimation of PSK-Modulated Carrier Phase with Application to Burst Digital Transmission, IEEE Trans. Inf. Theory, vol. IT-29, No. 4, pp. 543-551.
- [9] B. Vucetic and J. Nicolas, "Construction of MPSK Trellis Codes and Performance Analysis over Fading Channels", ICC'90, Atlanta, USA, April 1990.

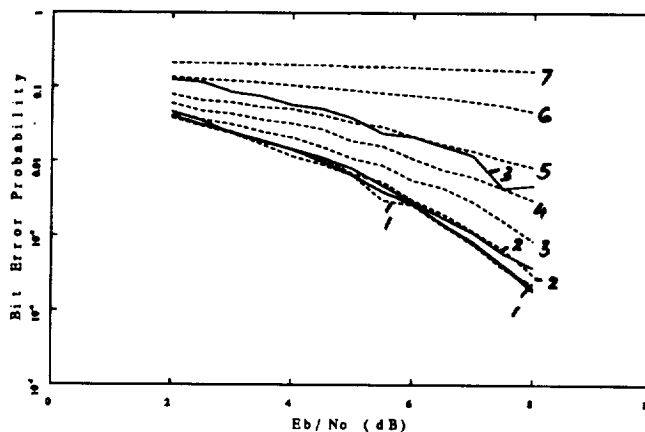


Figure 1: BER performance of QPSK with phase jitter on an AWGN channel:  
 Dash: without FFD; 1 to 7: 0, 5, 10, 15, 20, 30 and 40 degrees phase jitter  
 Solid: with FFD; 1: 5 to 20 degrees; 2: 30 degrees; 3: 40 degrees phase jitter

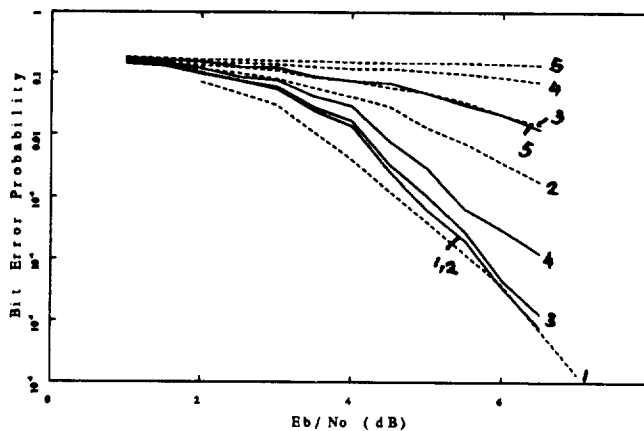


Figure 2: BER performance of TCM with phase jitter on an AWGN channel:  
 Dash: without FFD, Solid: with FFD ; 1 to 5: 0, 5, 10, 15 and 20 degrees phase jitter

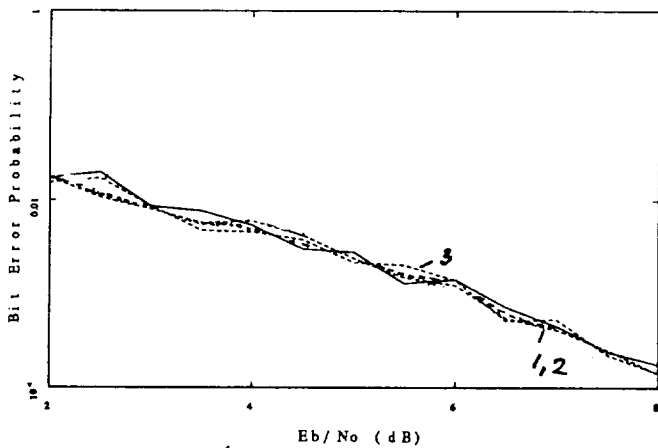


Figure 3: BER performance of the QPSK on an AWGN channel with phase jitter and DD scheme; Solid: Ideal QPSK; Dash: 1: phase jitter=10° 2: phase jitter=20° 3: phase jitter=30°

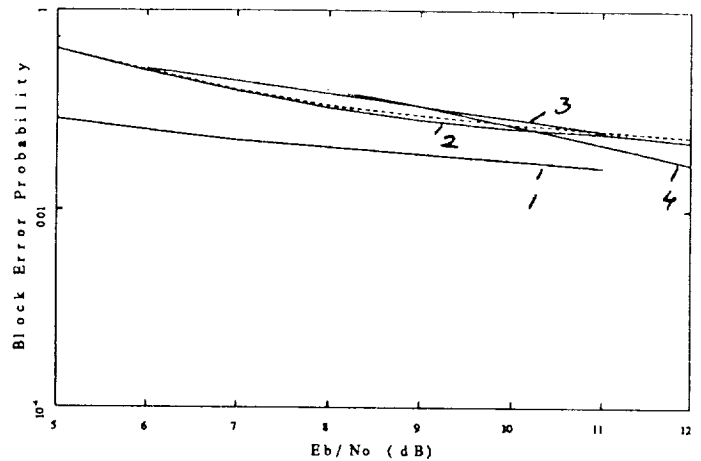


Figure 5: BLER performance of the QPSK modulation with the various carrier recovery schemes for experimental data; Dash: No carrier recovery; Solid: 1: TTIB 2: FF 3: DD 4: DD with preamble

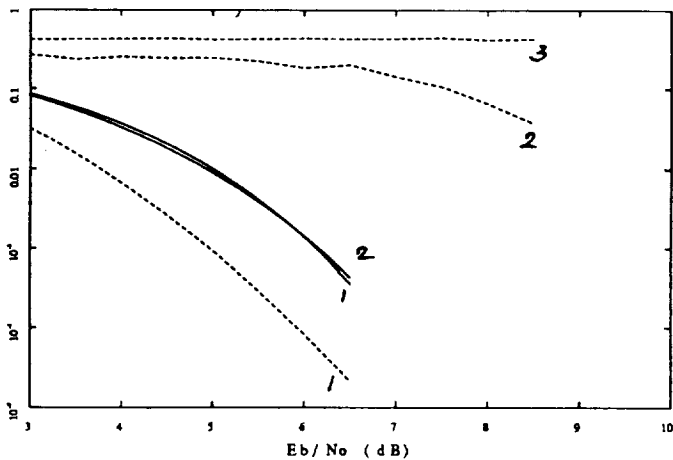


Figure 4: BER performance of the 16-state TCM code on an AWGN channel with phase jitter and TTIB scheme;  $\frac{B}{B'} = 50$  Dash: No phase recovery 1: phase jitter=0° Ideal TCM; 2: phase jitter=30° 3: phase jitter=50° Solid: TTIB 1: phase jitter=30° 2: phase jitter=50°

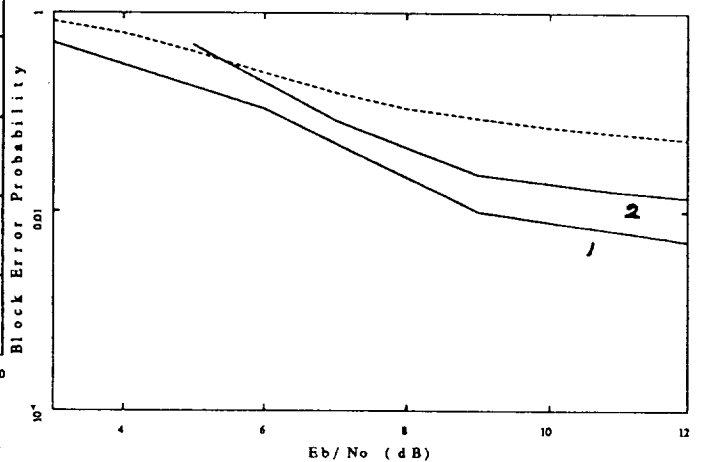


Figure 6: BLER performance of the 16state Ungerboeck TCM code carrier recovery for experimental data; Dash: Uncoded QPSK with ideal phase recovery; Solid: 1: TTIB 2: FF